

Search for Weakly Interacting Massive Particles with CDMS and XENON

Elena Aprile^{1,2}, Laura Baudis^{3,4}, Blas Cabrera^{5,6}

¹ Physics Department and Columbia Astrophysics Laboratory, Columbia University, New York, NY 10027, USA

³ Department of Physics, RWTH Aachen University, Aachen, 52074, Germany

⁵ Physics Department and KIPAC, Stanford University, Stanford, CA 94305, USA

E-mail: ¹ age@astro.columbia.edu, ³ laura.baudis@rwth-aachen.de,
⁵ cabrera@stanford.edu

Abstract. The Cryogenic Dark Matter Search (CDMS) and XENON experiments aim to directly detect dark matter in the form of weakly interacting massive particles (WIMPs) via their elastic scattering on the target nuclei. The experiments use different techniques to suppress background event rates to the minimum, and at the same time, to achieve a high WIMP detection rate. The operation of cryogenic Ge and Si crystals of the CDMS-II experiment in the Soudan mine has yielded the most stringent spin-independent WIMP-nucleon cross-section ($\sim 10^{-43}$ cm²) at a WIMP mass of 60 GeV/ c^2 . The two-phase xenon detector of the XENON10 experiment is currently taking data in the Gran Sasso underground lab and promising preliminary results were recently reported. Both experiments are expected to increase their WIMP sensitivity by a one order of magnitude in the scheduled science runs for 2007.

1. Introduction

Recent observations from high-redshift supernovae [1, 2, 3], cosmic microwave background anisotropy measurements [4, 5], the red-shift galaxy clusters [6], and the Sloan Digital Sky Survey [7] provide growing evidence that the mass in the Universe is dominated by dark matter, which is non-luminous, non-baryonic and could be weakly interacting massive particles (WIMPs) [8]. One attractive candidate for WIMPs is the lightest supersymmetric particle (LSP) from supersymmetry models [9]. A WIMP can deposit a small amount of energy (a few tens of keV) in an elastic scattering with an atomic nucleus [10], with a rate much less than 1 event/kg/day.

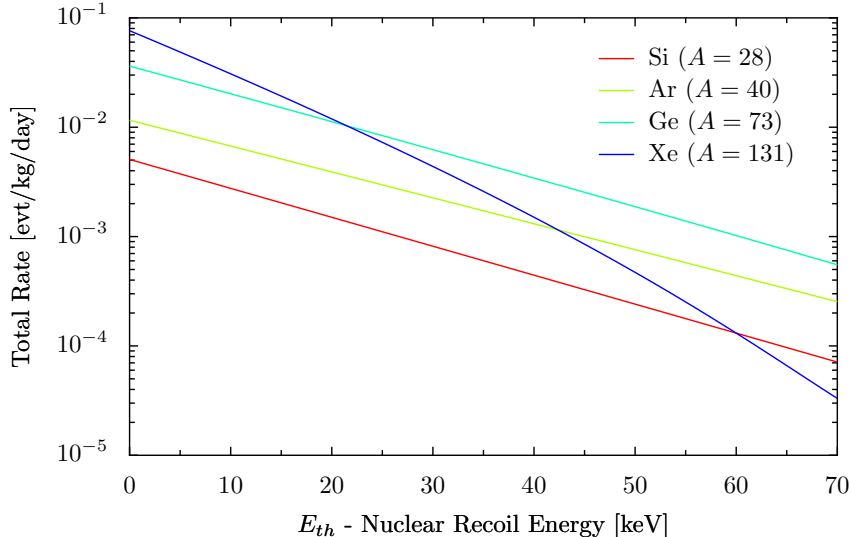
Figure 1 shows the predicted event rates for a WIMP mass of 100 GeV/ c^2 and a spin-independent WIMP-nucleon cross-section of 10^{-43} cm² for different target materials, according to [11]. It can be seen that the event rate falls quickly at high recoil energy. A low energy-threshold (~ 10 keV) is one of the key requirements for direct dark matter search experiments, such as CDMS and XENON, to achieve a good WIMP detectability. While the WIMP detection rate on xenon (the target material for XENON experiment) is suppressed at large recoil energies (we use the nuclear form factor by [12]), it is enhanced at low recoil energies by the large atomic

² On behalf of the XENON collaboration

⁴ On behalf of the CDMS and XENON collaborations

⁶ On behalf of the CDMS collaboration

Figure 1. Calculated WIMP detection rate as a function of detector energy-threshold E_{th} for four different target materials (Xe, Ge, Ar and Si). A WIMP mass of $100 \text{ GeV}/c^2$ and WIMP-nucleon cross-section of 10^{-43} cm^2 are used.



mass of xenon. From figure 1, the event rate in the Xe detector is about 30% higher than for Ge, for an energy threshold of 10 keV. The CDMS experiment uses both Ge detectors for high WIMP sensitivity ($\times 6$ better than Si) and Si detectors for added neutron rejection with the same neutron rate as Ge.

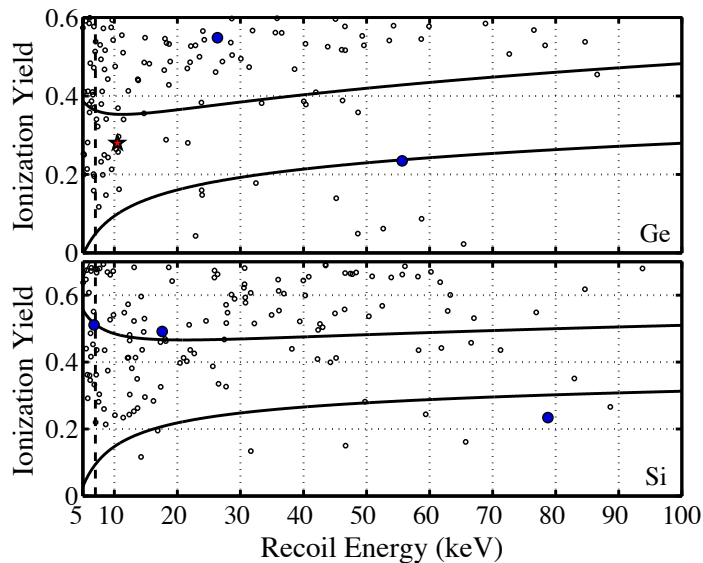
2. CDMS-II Experiment

The CDMS-II experiment (a detailed description of the experimental apparatus can be found in [13]) is located in one of the two excavated caverns of the Soudan Underground Laboratory, at a depth of 780 m (2090 m.w.e. or meter-water-equivalent). The surface muon flux is reduced at the underground lab by a factor of 5×10^4 . An additional active muon veto shield, consisting of 5-cm-thick BC-408 plastic scintillator slabs, is used to tag cosmic ray muons. A passive shield, consisting of 40-cm-thick outer polyethylene, 22.5-cm-thick lead (including 4.5-cm-thick inner ancient lead), and 10-cm-thick inner polyethylene, is enclosed by the muon veto and houses the detectors. The passive shield reduces most of the gamma-ray and neutron background from radioactivity in the surrounding rock or produced by cosmic ray muons interacting with the surrounding rock and shield. To reduce the radon activity in the vicinity of the detectors, medical grade breathing air is used to purge the space inside of the Pb shield continuously.

At the core are Z(depth)-sensitive ionization and phonon-mediated (ZIP) detectors, kept at a base temperature below 50 mK. Each ZIP detector is a cylindrical high-purity Ge (250 g) or Si (100 g) crystal. Two concentric ionization electrodes and four independent phonon sensors are photolithographically patterned onto each crystal. A particle interacting in a ZIP detector causes either an electron recoil (gamma rays, electrons, neutron inelastic scattering, etc.) or a nuclear recoil (neutron elastic scattering, WIMPs). The interaction deposits its energy into the crystal through charge excitations (electron-hole pairs) and lattice vibrations (phonons). The charge excitations are collected with electrodes on the two sides of the ZIP detector. The electron-equivalent energy E_Q is equal to $N_Q \times \epsilon$, where N_Q is the number of collected charges and ϵ is the average energy needed to produce an electron-ion pair ($\epsilon \approx 3 \text{ eV}$ in Ge and 3.8 eV in Si). The phonon signal is detected by quasiparticle-trap electrothermal-feedback transition-

edge sensors (QETs) photolithographically patterned onto one of the crystal faces. Since the drifting of electrons and holes across the crystal also contributes the phonon signal, the recoil energy E_R of an event is inferred from both the phonon and ionization signals. E_Q is equal to the recoil energy E_R for electron recoils. Nuclear recoils produce less electron-ion pairs, which makes E_Q less than E_R . Thus the ionization yield, defined as $y = E_Q/E_R$, is much smaller for nuclear recoils ($y \sim 0.3$ for Ge and ~ 0.25 for Si above 20 keV) than that for electron recoils ($y = 1$). It provides the technique to reject the electron-recoil events which produce most of the background.

Figure 2. Ionization yield versus recoil energy for events in the CDMS-II (top - Ge, bottom - Si) detectors, before the timing cut for removing the surface electron recoil events. The curved lines represent the defined WIMP signal regions with an energy-threshold at 7 keV (dashed vertical lines). After the cut, one event (star, red) remains in the signal region for the Ge data, while no candidate event is seen for the Si data. Figure from [14].



The CDMS-II experiment has been operating in the Soudan mine since October 2003 and reported their recent results, from WIMP search data collected through August 2004 with a total of 74.5 live days exposure, yielding a total spectrum-weighted exposures of 34 (12) kg d for the Ge (Si) targets in the 10-100 keV nuclear recoil region [14]. Analysis was performed blindly by masking the events from the candidate region, defined by using calibration data from ^{133}Ba and ^{252}Cf sources and from non-masked WIMP search data. The ZIP detector provides excellent event-by-event discrimination of nuclear recoils from background electron recoils in the detector's bulk region. However, electron recoils near the detector's surface suffer from poor ionization collection and leak into the candidate nuclear recoil region. New analysis techniques were developed to remove those surface electron recoils. The phonon pulses from surface recoils are more prompt than those recoils in the detector bulk. A timing parameter, defined as the sum of the time delay of the phonon signal relative to the fast ionization signal and the phonon rise time, was used to reject the surface electron recoils. One candidate event was found after unmasking the Ge WIMP search data (figure 2 top). However, that event occurred in a time period when the detector suffered inefficient ionization collection. It is also consistent with the rate of expected background. The expected number of surface events after the timing cut is $0.4 \pm 0.2(\text{stat}) \pm 0.2(\text{sys})$ between 10-100 keV in Ge. The expected neutron background that

escapes the muon veto is 0.06 events in Ge. No candidate event was found in the Si data (figure 2 bottom). Based on these data and previous results from Soudan [15], a 90% C.L. upper limit on the spin-independent WIMP-nucleon cross section is $1.6 \times 10^{-43} \text{ cm}^2$ from Ge and $3 \times 10^{-42} \text{ cm}^2$ from Si, for a WIMP mass of $60 \text{ GeV}/c^2$.

The experiment is now operating five towers (21 Ge and 9 Si ZIP detectors) with more than 4 kg of Ge and 1 kg of Si and is expected to reach a sensitivity down to $2.1 \times 10^{-44} \text{ cm}^2$ for spin-independent WIMP-nucleon cross section at $60 \text{ GeV}/c^2$ by the end of 2007. In addition, plans are underway for the construction and operation at SNOLAB of the SuperCDMS 25 kg Experiment, which will operate 25 kg of Ge for three years with a target sensitivity of 10^{-45} cm^2 for $60 \text{ GeV}/c^2$ WIMPs.

3. XENON10 Experiment

XENON10 is a dual phase (liquid/gas) xenon time projection chamber (TPC) located in the Gran Sasso Laboratory in Italy (3500 m.w.e). The total muon flux is about $1 \text{ /m}^2/\text{hr}$, one order of magnitude lower than that in the Soudan mine. The detector is installed in a passive shield consisting of a 20-cm-thick outer layer of Pb (including 5 cm inner layer of low-activity Pb) and 20-cm-thick inner layer of polyethylene, reducing the external gamma flux by a factor of 10^5 and the neutron flux by a factor of at least 100 [16]. Radon purge from N_2 gas is used in the shield continuously. The background rate from ^{85}Kr contamination (25 ppm in natural Xe) is reduced by a factor of 5000 by using a commercially available low- ^{85}Kr (5 ppb) xenon, contributing negligible rate compared to the background rate from the detector materials. The XENON10 TPC is filled with 22 kg of ultra pure liquid xenon (LXe). The active volume is defined by a Teflon cylinder with an inner diameter of 20 cm and a height of 15 cm for a total active mass of 15 kg of LXe. The TPC is equipped with four wire meshes, two in the liquid and two in the gas. The bottom mesh serves as cathode and the next one, positioned just below the liquid level, together with a series of field shaping rings, form the 15 cm drift region. The two last meshes, together with the one below the liquid level, serve to define the gas proportional scintillation region.

Figure 3. Total waveform for a typical gamma event.

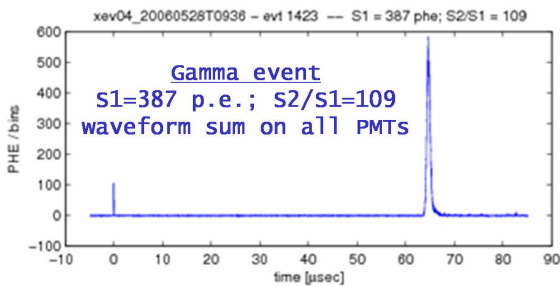
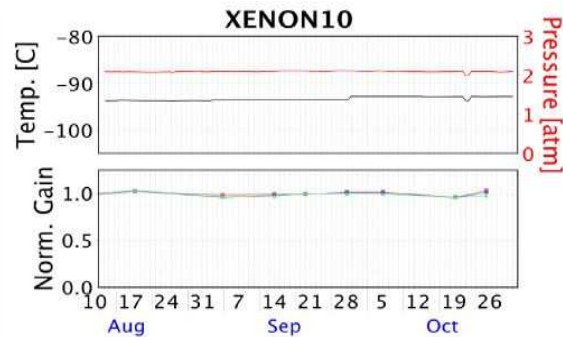


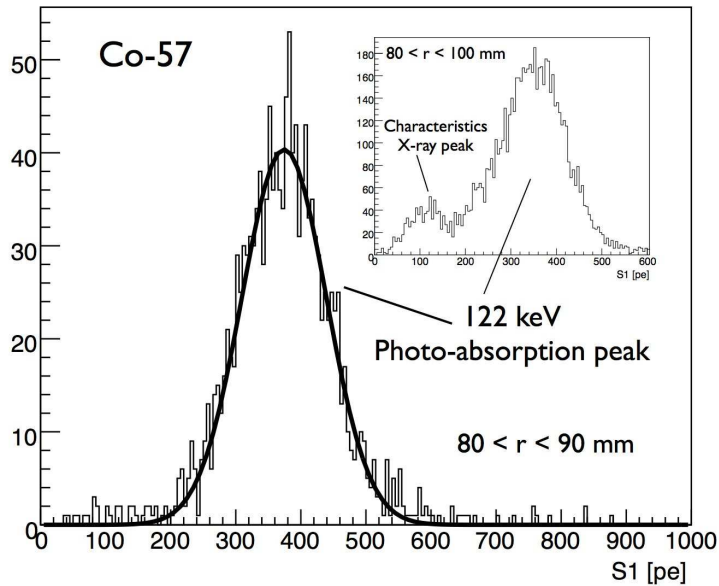
Figure 4. XENON10 detector's pressure, temperature and PMT gains during operation.



The electron/nuclear recoil from a particle interaction produces excitation (Xe^*) and ionization (electron-ion pair $\text{Xe}^+ + e^-$) in the liquid. The excited Xe molecules decay and produce scintillation light in the UV range (175 nm). The XENON experiment uses UV-sensitive photo-multipliers (PMTs) to detect the prompt light signal (also called primary light, or $S1$). The electron-ion pairs recombine and form excited states, which also contribute to $S1$. By applying an electric field ($\sim 1 \text{ kV}/\text{cm}$) in LXe, part of the ionization electrons can be liberated

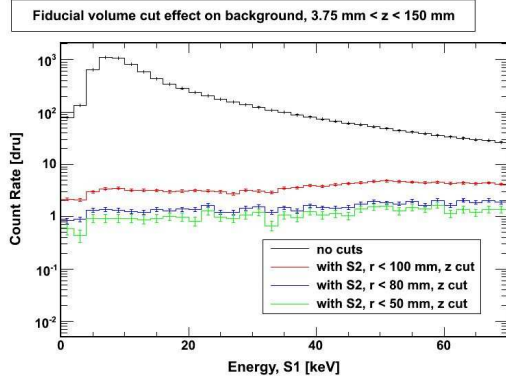
from recombination. Those electrons drift to the liquid-gas interface, are extracted into the gas, where they produce secondary excitation with a gain of a few hundred [17] in a strong electric field (~ 10 kV/cm). The scintillation light from the secondary excitation in the gas is also detected by the PMTs as a delayed signal (also called secondary light, or $S2$). The two-phase operation allows detection of a single ionization electron from one event. Due to the difference in stopping power and ionization density of electron and nuclear recoils in LXe, the ratio of ionizing electrons escaping the electron-ion recombination is different, resulting in smaller $S2/S1$ values for nuclear recoils [18].

Figure 5. S1 scintillation spectrum from ^{57}Co calibration.



The active XENON10 volume is viewed by 89 Hamamatsu R8520-06-A1 1" square PMTs, 35 mm high. The bottom array of 41 PMTs is located below the cathode, fully immersed in LXe, to detect the S1 light signal. The 48 PMTs of the top array, in the gas, are used to detect the proportional ($S2$) light signal. A typical low energy gamma event is shown in figure 3. The time separation between the two pulses of direct and proportional light, (maximum $75 \mu\text{s}$ determined by the 15 cm drift and the $2\text{mm}/\mu\text{s}$ electron drift velocity) provides the event depth of interaction in the liquid (or z -coordinate). Cooling for the XENON10 detector is provided by a Pulse Tube Refrigerator mounted on the cryostat top flange, directly in contact with the Xe gas. Figure 4 shows the remarkably stable pressure ($\Delta P < 0.006$ atm) and temperature ($\Delta T < 0.005^\circ\text{C}$) values of XENON10 for over three months of operation underground. Under such stable conditions the fluctuation of PMT gains is $< 2\%$. The light yield in XENON10, depends on event energy and position. Measurement of this yield has been carried out with gamma sources. In the bulk region ($radius < 5$ cm), the 662 keV photo-absorption peak of ^{137}Cs gives an average light yield of 1464 photo-electrons (pe) (2.2 pe/keV) and a sigma of 205 pe (14%). The light yield does not change substantially (less than 5%) for $radius < 9$ cm. Figure 5 shows a scintillation light spectrum from a ^{57}Co calibration, after drift time corrections. For a $radius$ between 8 and 9 cm, the average light yield for 122 keV gamma rays is 374 pe (3.1 pe/keV), with a resolution of 17% (σ). The higher light yield from the 122 keV gamma rays is partly due to the different electron-ion recombination contributions for different energy gamma rays in LXe [19]. The insert in figure 5 shows the clear detection of the characteristic X-ray peak due to K -shell electrons (30 keV).

Figure 6. Background energy spectrum in XENON10, before and after selecting events with both light and charge signal and after fiducial volume cuts.



An important background rejection feature of the XENON10 detector is the ability to localize events in three dimensions (3D) with a good resolution. Since electron diffusion in LXe is small, the S2 pulse is produced in a small region with the same xy coordinates as the interaction site, allowing xy localization with an accuracy of a few mm. With the more precise z information (better than 1 mm) from the drift time measurement, the 3D event localization provides powerful background discrimination via fiducial volume cuts. The total background rate in XENON10, including events with only an S1 signal from interactions in the “passive” LXe outside the sensitive volume, is shown in figure 6 (black curve). By requiring also a single S2 signal and with only a few millimeter z -cut from above, the rate in the sensitive volume is reduced by three orders of magnitude at 10 keV (red curve). This demonstrates the efficient self shielding effect of liquid xenon. The rate can be further reduced by a factor of 2 by using the xy event localization and removing events in the outer 5 cm of LXe (green curve). The achieved XENON10 energy threshold is less than 10 keVr with a light yield of about 1 pe/keVr, taking into account the measurement of the scintillation efficiency of Xe recoils in LXe [20].

Monte Carlo simulations, using the GEANT4 software package, were carried out to understand the background sources in XENON10. As shown in figure 7, the measured background rate can be explained by the radioactivity in the PMTs, the stainless steel used in the detector and cryostat, and the signal and high voltage ceramic feedthroughs.

The statistics of the dark matter search data accumulated to-date amounts to more than 30 days of live time. Figure 8 shows a plot of $\log_{10}(S2/S1)$ as a function of energy for 22.2 live days, giving a total exposure of 38 kg d after cuts. The magenta line corresponds to the centroid of the electron recoil band while the green one corresponds to the centroid of the nuclear recoil band, from measurements with smaller XENON prototypes [18, 21]. In the electron equivalent energy region 3-16 keVee (corresponding to a recoil energy region of 10-40 keVr), zero events are observed in the 50% acceptance window of the nuclear recoil band. Assuming the nuclear recoil band as measured with the small prototypes, the preliminary XENON10 sensitivity to WIMP-nucleon spin independent cross section is about $2.0 \times 10^{-43} \text{ cm}^2$ at 100 GeV/ c^2 WIMP mass. Currently, the XENON10 detector continues to accumulate WIMP search data in stable operation mode. A neutron calibration run at the Gran Sasso laboratory is scheduled for the first week of December 2006. Small upgrades and replacement of know radioactively ‘hot’ components in the detector are planned for January 2007. The new run to start in 2007 will allow XENON10 to explore the WIMP-nucleon cross section down to the 10^{-44} cm^2 region, as shown in figure 9.

Figure 7. Comparison of XENON10 background data with Monte Carlo background data from radioactivity in the PMTs, ceramic and stainless steel detector components.

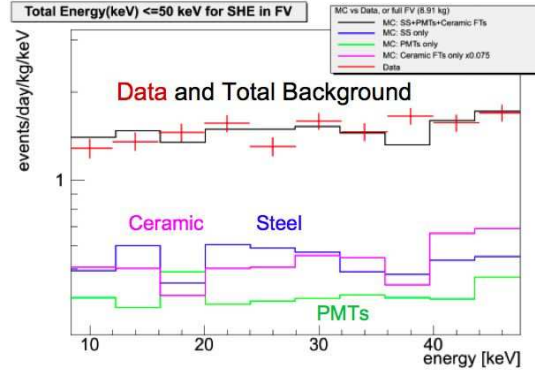


Figure 8. XENON10 ionization yield versus energy. The magenta and green lines correspond respectively to the centroid of the ER and the NR bands.

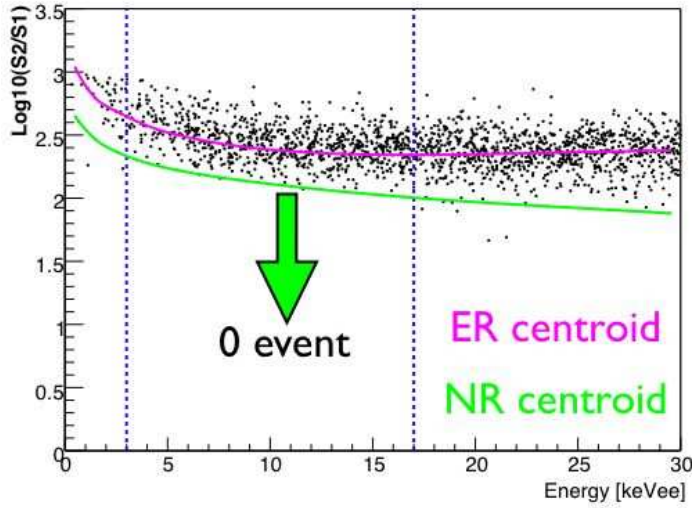
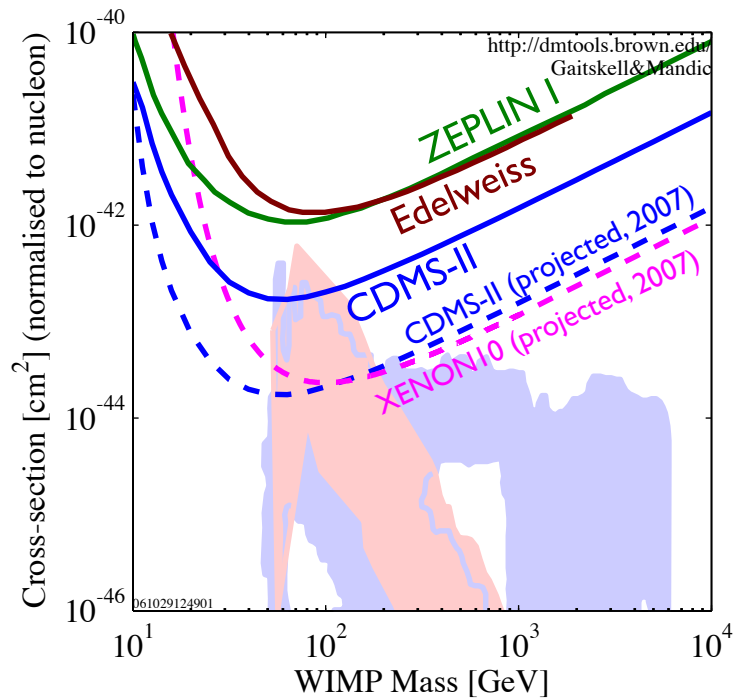


Figure 9. WIMP-nucleon cross-section upper limit (90% C.L.) from direct dark matter search experiments CDMS [14], Edelweiss [22] and ZEPLIN I [23]. The projected upper limits from CDMS-II and XENON10 experiments in 2007 are shown as dashed lines. The shaded areas are allowed parameters from some supersymmetry models [24, 25].



4. Summary

The development of low radioactive, low energy-threshold, and high background discrimination detectors by the CDMS and XENON collaborations provides promising ways to explore new physics by searching for dark matter particles via their direct elastic scattering in terrestrial targets. The recent CDMS result starts to exclude parameter space from constrained (mSUGRA - minimal supergravity) supersymmetry models, as shown in figure 9. The XENON10 experiment is expected to report first results from the current science run in 2007. Both experiments should reach a factor of 10 increase in sensitivity with respect to the current CDMS level by the end of 2007.

References

- [1] Perlmutter S *et al.* 1999 *Astrophys. J.* **517** 565
- [2] Knop R A *et al.* 2003 *Astrophys. J.* **598** 102
- [3] Astier P *et al.* 2006 *Astron. Astrophys.* **447** 31
- [4] Spergel D N *et al.* 2003 *Astrophys. J. Suppl.* **148** 175
- [5] Spergel D N *et al.* 2006 Wilkinson microwave anisotropy probe (wmap) three year results: Implications for cosmology (*Preprint arXiv:astro-ph/0603449*)
- [6] Peacock J A *et al.* 2001 *Nature* **410** 169
- [7] Tegmark M 2004 *Phys. Rev. D* **69** 103501
- [8] Lee B W and Weinberg S 1977 *Phys. Rev. Lett.* **39** 165
- [9] Jungman G, Kamionkowski M and Griest K 1996 *Phys. Rept.* **267** 195
- [10] Goodman M W and Witten E 1985 *Phys. Rev. D* **31** 3059
- [11] Lewin J D and Smith P F 1996 *Astropart. Phys.* **6** 87
- [12] Engel J 1991 *Phys. Lett. B* **264** 114
- [13] Akerib D S *et al.* 2005 *Phys. Rev. D* **72** 052009
- [14] Akerib D S *et al.* 2006 *Phys. Rev. Lett.* **96** 011302
- [15] Akerib D S *et al.* 2004 *Phys. Rev. Lett.* **93** 211301
- [16] Sorensen P 2006 Xenon10: Dark matter direct detection, a talk presented at the 6th international workshop on the identification of dark matter (idm 2006), rhodes, greece, september 2006
- [17] Bolozdynya A I 1999 *Nucl. Instr. and Meth. A* **422** 314
- [18] Aprile E *et al.* 2006 *Phys. Rev. Lett.* **97** 081302
- [19] Yamashita M *et al.* 2004 *Nucl. Instrum. Meth. A* **535** 692
- [20] Aprile E *et al.*
- [21] Shutt T, Dahl C E, Kwong J, Bolozdynya A I and Brusov P 2006 Performance and fundamental processes at low energy in a two-phase liquid xenon dark matter detector (*Preprint arXiv:astro-ph/0608137*)
- [22] Sanglard V *et al.* 2005 *Phys. Rev. D* **71** 122002
- [23] Alner G J *et al.* 2005 *Astropart. Phys.* **23** 444
- [24] Baltz E A and Gondolo P 2004 *JHEP* **0410** 052
- [25] Ellis J R, Olive K A, Santoso Y and Spanos V C 2005 *Phys. Rev. D* **71** 095007